

The impedance of 23Ah Ni-Cd cells with sintered electrodes: measurements in the range 10 kHz–0.001 Hz as an indication of residual capacity

M. HUGHES, R. T. BARTON, S. A. G. R. KARUNATHILAKA, N. A. HAMPSON, R. LEEK

Department of Chemistry, University of Technology, Loughborough, Leics. LE11 3TU, UK

Received 9 January 1984; revised 10 May 1984

Impedance measurements on 23 Ah Ni–Cd cells at various residual capacity levels are described. These have been made using non-inductive connections coupled directly to a potentiostat and a frequency response analyser.

The capacitive reactance at 0.39 Hz provided the best residual capacity indicator.

1. Introduction

The impedance of two-terminal primary cells has been studied in connection with the estimation of the residual capacity. The results of this research have been described in detail by Hampson *et al.* [1] and more briefly [2]. The estimation of the state-of-charge of secondary cells, particularly those of commercial importance, is an important problem which, in spite of much research, has not yet been solved. The lead-acid cell is *prima facie* a simpler system to treat than the nickel–cadmium cell as a consequence of the electrolyte density changes which occur as charge is removed from the cell (even with this there are many applications in which density determinations cannot be made conveniently). The nickel–cadmium cell electrolyte remains effectively constant throughout the discharge so that even this possible quantity is useless for prediction. Coupled with the state-of-charge problem is the state-of-health problem in which the deterioration of the cell quality requires prediction. It is a logical extension of our work on impedance as a method for the estimation of the state-of-charge of primary cells to investigate the impedance method as a possible tool for the evaluation of the quality and the state-of-charge of secondary cells. Of the commercially important secondary cells the nickel–cadmium cell was first chosen for this extension since this was the one

for which there was the most pressing need for a residual capacity test.

It was known that the potentials of the industrial electrodes of nickel–cadmium cells do not change in a useful way with state-of-charge [3]. Charge–discharge characteristics are not sufficiently well defined to produce a satisfactory test and redox dye methods were unstable [4]. Polarization of cells during charge and discharge has been intensely investigated [5, 6]. Indeed, Kordes had built a device for monitoring the state-of-charge but it was found not to be a suitable battery tester [7]. A more recent test device based on a ‘current-sharing with a test battery’ technique has been described [8]. These workers found that both the ion specific (K^+) electrode and the cell phase shift were incapable of yielding reliable tests [9]. More recently, Sathanarayana *et al.* [9] have claimed that the state-of-charge can be predicted if the equivalent cell capacitance or the a.c. phase shift is measured at a test frequency in the range 5–30 Hz. These results were explained by the assumption that the rate controlling reaction under their test conditions was diffusion into solution. A more recent paper by Zimmerman *et al.* [10] agrees that diffusion processes are rate controlling; one of these diffusion processes is apparently a solid-state one in a surface film. The diffusion characteristics are claimed to be dependent upon the state-of-charge. In the present work

we have followed the pattern used in our earlier investigation; this paper records our results.

2. Experimental details

The battery of cells used for the experiments was a nominal 23 Ah unit which was originally intended as a 25 V aircraft battery. The unit was obtained after seven years service in a conventional mode followed by approximately 6 months open circuit storage. The unit was charged according to the manufacturer's instructions and BS 2G-205: 1976. When tested according to instructions individual cells generally yielded in excess of their rated capacity at the C rate; however, there was some variation in capacities when tested by successive discharges. The cells were considered to be satisfactory for the present purposes. In general the testing procedure was to fully charge the cells and carry out impedance testing after definite quantities of charge had been removed. The residual charge of the cell was calculated on the basis of the total quantity of charge which could be delivered by the cell and not on the nominal capacity of the cell.

2.1. Connections to the impedance measuring equipment

As has become customary in contemporary electrochemistry, connections to the impedance estimation equipment (SOLARTRON 1170) were made via a suitable potentiostat. From our initial results, it was clear that the lead and connector impedances were significant in comparison with the faradaic impedance of the cell. The main reason for this conclusion was that not only did the impedances not change with discharging in the expected way but the behaviour was erratic. This observation did not correspond with our experience and expectation of cells of this quality. Fig. 1 shows examples of impedance loci of cells measured with 30 cm leads at nominally 100 and 0% state-of-charge.

The connections within the cell were possibly a cause of this; however, our experience with the leads argued against these mechanical sources. We were forced to conclude that the 1186 was not suitable for this particular study. The availability of a second 1186 interface allowed a

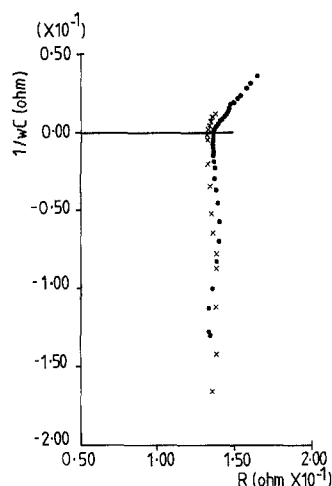


Fig. 1. Impedance spectra of a 23 Ah Ni-Cd cell. $\times - 100$, $\bullet - 0\%$ states-of-charge using 30 cm wires and crocodile clips in the frequency range 10 kHz–1 mHz–10 points per decade.

check on our original interface; both behaved identically.

A Kemitron potentiostat was substituted for the 1186 interface. The cell potential was measured directly from the terminals onto the voltage input of the Frequency Response Analyser (FRA). The current was measured by the voltage developed across an accurately standardized low resistance (26.54 mohm). Fig. 2 shows the impedance spectra of (a) a fully charged and (b) a fully discharged cell. These results indicate that the true cell impedance is a tenth of the value obtained when measured with the 1186. It should be noted that tests on standard low impedances fully justified our conclusions.

Matters were further improved by standardizing the lead-to-cell connections. Initial data had

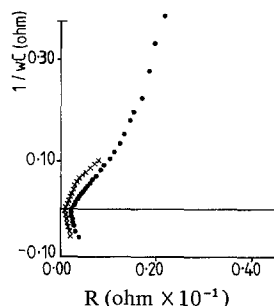


Fig. 2. Impedance spectra of a 23 Ah Ni-Cd cell. $\times - 100$, $\bullet - 0\%$ states-of-charge using non-inductive connections and the Kemitron potentiostat in the frequency range 10 kHz–1 mHz.

also shown that there was a random variation in the resistive component at zero (ωL) at different states-of-charge. It was therefore decided to optimize the torque on the nuts and to use that (fixed) torque in subsequent experiments. This was optimized at 60 f lb in^{-1} . It was apparent that by introducing this constant torque on the connecting nuts, the cell-to-cell variation, was eliminated and any poor lead-to-cell connections were identifiable and could be remedied. After minimizing the large inductances, the true cell impedance could be investigated after the cells had been subjected to a range of tests.

3. Results

3.1. The impedance spectrum of a fully charged cell

The impedance spectra of a fully charged cell are shown in Fig. 3. The spectra of such cells are very reproducible and represent a complicated electrochemical system. On several previous occasions we have been able to attribute the resulting spectrum to one or the other electrode. It is clear that we cannot do the same thing here as both electrodes have impedance components of approximately equal magnitude [11] and thus make equal contributions to the total cell impedance.

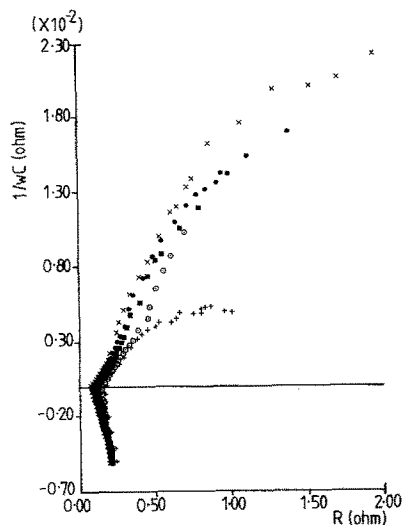


Fig. 3. Impedance spectra of a 23 Ah Ni–Cd cell fully charged taken 1 hr after charging in the frequency range 10 kHz–1 mHz.

The spectra consist of a small inductive component and a capacitive component in which the loci make an angle of approximately 70° to the real axis. At low frequencies (4 mHz) the locus curves over slightly.

The high dihedral angle and the curving of the locus at low frequencies indicates the presence of blocking films which are due to $\text{Cd}(\text{OH})_2$ [11]. This picture is qualitatively constant regardless of the previous history of the cell; the second order difference in the curves probably reflect the extent of the blocking films of $\text{Cd}(\text{OH})_2$.

3.2. Variation of new cell on standing

3.2.1. Variation of the impedance spectra of a fully charged cell on standing. A fully charged cell was taken and the changes in its impedance spectrum over a period of 120 days were monitored. Some of the resulting spectra are shown in Fig. 4. Such changes as occur in the spectra are only apparent below 49 mHz but, because they are so varied, they cannot be systematized. Above this frequency the spectra taken at different times are very similar consisting of a small inductive component approximately 6 mohm and a capacitive component in which the loci subtend an angle of about 72° to the real axis. In this connection it is

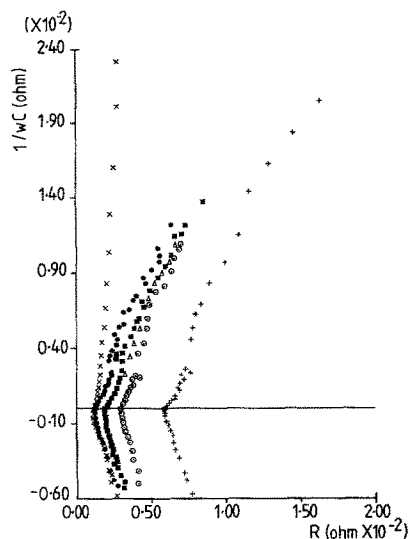


Fig. 4. Variation in the impedance spectra of a fully charged cell on open circuit standing after: X – 24, O – 52, ■ – 76, ● – 84, + – 88 days in the frequency range 10 kHz–1 mHz.

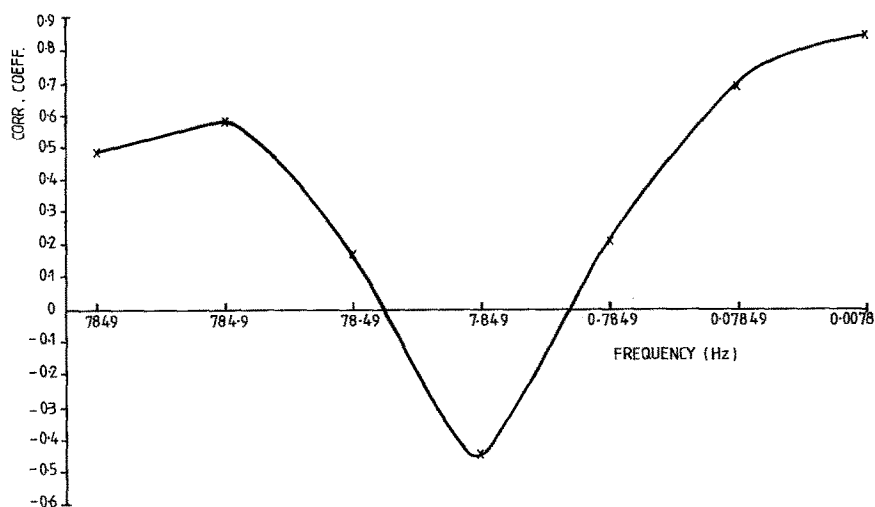


Fig. 5. Variation in the capacitive reactance correlation coefficient with time at different frequencies.

noteworthy that there is no evidence to support the view of an increase in the amount of film deposited on the surface of the electrodes as they self-discharge even as a result of 120 days open-circuit stand.

The only parameter to show any marked change in the correlation coefficient with time as the cell self-discharged, was the capacitive reactance at 7 mHz as shown in Fig. 5.

3.2.2. Self-discharge of a nominally fully charged and a 50% charged cell: voltage measurements. The open circuit voltage of the cell tested

above, together with the open circuit voltage of a cell 50% charged were monitored over a period of 120 days. The resulting voltage vs time curve is shown in Fig. 6. We can conclude from this experiment that a fully charged cell retains its capacity for a longer period than the partially discharged cell. The rate at which the OCV of the partially discharged cell decreases is seen to increase as the time increases, whilst for the fully charged cell the rate of self-discharge is apparently constant, being about $0.0005 \text{ mV day}^{-1}$ which represents a self-discharge of $\sim 0.05\%$ per day.

The voltage vs time curve is analogous to that

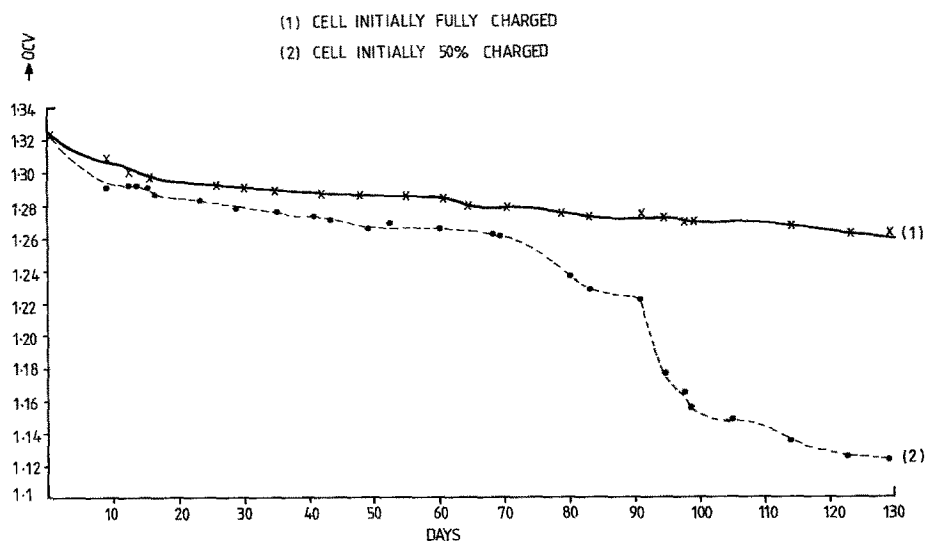


Fig. 6. Variation in the open circuit voltage of (1) a fully charged and (2) a cell 50% charged with time.

shown in a cell discharged at any rate. The only differences are in the time duration over which the discharge is carried out and in the rate at which the cell voltage falls. When a cell is discharged, as the state-of-charge falls, so the rate at which the voltage falls increases. This is precisely what has occurred in the cell 50% charged, whose rate of self-discharge is approximately 6 times faster than the fully charged cell, being about 0.3% per day.

Of interest is the sudden voltage decrease observed in the partially discharged cell after 90 days. The reason for this is not clear, but it is unfortunate that these changes are not reflected in the impedance spectra.

3.3. Cell and cell-to-cell variation

Before we standardized the leads from the cell to the FRA we had gross changes in the impedance spectra between the cells and in the single cell variations under identical conditions.

The process of standardizing the connections resulted in the inductive reactance becoming constant in all the cells studied irrespective of what tests had been carried out on them. This shows that the inductive reactance has no electrochemical origins but is most probably a contribution from the leads used. We found that there was good replication between cells discharged at different rates in the frequency range down to 49 mHz. Only below this frequency, when the integration time was minimized, were there any significant differences in the spectra. Tests also showed no difference in the impedance spectra of the cell when it was discharged at rates between the C1 and C4.6 in the frequency range down to 49 mHz. At lower frequencies, the results of the tests on cells and replicates on the same cell were not reproducible. At higher frequencies, the spectra of cells discharged at different rates were practically identical. The variation in the resistive component between cells is minimal. As the resistive component did not change as the cells were discharged, it is apparent that the use of the cell resistance as a state-of-charge indicator is inadmissible. Similarly, since there are only insignificant changes in the impedance spectra of the cells discharged at different rates and in a stepwise or a non-stepwise manner at all residual

charges (excluding 100% discharged) in the frequency range down to 49 mHz, they cannot be sufficiently resolved for use as a residual charge indicator. Attempts to find a simple residual charge indicator based on the deconvoluted data obtained from frequencies less than 49 mHz proved fruitless, as the results of tests on cells and replicates of the same cell were not reproducible.

3.4. Variation of impedance spectra with residual charge at different rates of discharging

The cells were discharged in a stepwise or non-stepwise manner by nominally 10% of their rated capacity at different rates of discharge, and an impedance spectrum taken after a one-hour equilibration period.

3.4.1. Stepwise discharge. By stepwise we mean discharging 100 → 90 → 80 and not 100 → 90, 100 → 80% C.

Typical impedance spectra of cells discharged in such a manner and at the C4.6 and C1.4373 rates are shown in Figs. 7 and 8. All of the spectra are similar in the frequency range down to 49 mHz and are identical to those already described for a fully charged cell (see Section 3.1.).

The absence of a well-defined high frequency

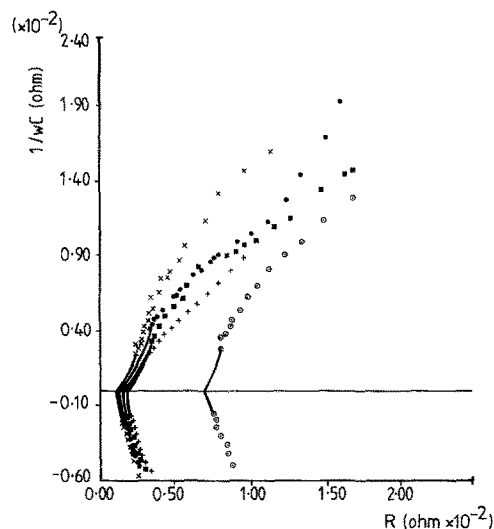


Fig. 7. Variations in the impedance spectra of a cell at: \times – 80, \bullet – 0, \circ – 40, $+$ – 60, \blacksquare – 50% states-of-charge, in the frequency range 10 kHz–1 mHz, discharged at the 5A, C4.6 rate, in a stepwise manner. Continuous line denotes multiple points.

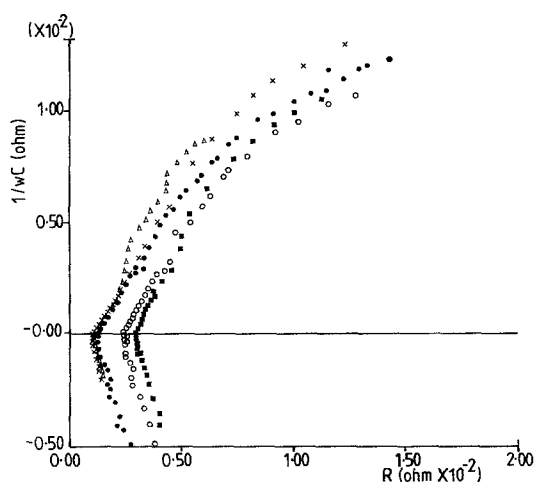


Fig. 8. As for Fig. 7 but discharged at the 16A C1.4375 rate, in a stepwise manner in the frequency range 10 kHz–1 mHz. \triangle – 60, \times – 80, \bullet – 40, \blacksquare – 50, \circ – 70% states-of-charge.

charge transfer process at both high and low rates of discharge indicates that the electrode kinetics are fast.

3.4.2. Discharge at the 5A C4.6 rate. There are no gross changes in the impedance spectra of this cell as charge is removed in a stepwise manner. However, some small changes occur:

(a) At most states-of-charge the dihedral angle which the loci make to the real axis is about 75 – 82° . At high states-of-charge, the dihedral angle is 80° , whilst at intermediate states-of-charge the angle decreases slightly to about 74° at 50% state-of-charge, and then increases to 82° when the cell is fully discharged.

(b) At low frequencies, less than 10 mHz, the loci bend over towards the real axis.

(c) When the cell was fully charged, 90% charged, 60% charged and 10% charged, at frequencies below 100 Hz, the dihedral angle which the loci made to the real axis was originally between 43 and 55° , which soon relaxed into another linear portion between 50 and 84° .

These results taken together show that at low discharge rates there is a massive build-up of resistive surface films probably of $\text{Cd}(\text{OH})_2$. As the cell is discharged the dihedral angle decreases slightly indicating that only a small disruption in the surface film occurs as the cell is discharged. As the cell is further discharged there is a continued

build-up of $\text{Cd}(\text{OH})_2$ films on the surface of the electrodes and there is an increase in the dihedral angle. The fact that the loci bend over towards the real axis at all states-of-charge is further evidence for the presence of films.

The fact that there is no evidence for a charge transfer process even at low states-of-charge where there are large film deposits on the electrode must indicate either:

(a) that the electrode reaction is not limited by the diffusion of the ions through the resistive films, or

(b) that as the discharge continues, there is a morphological or structural change which causes a redistribution of the surface films as the reaction penetrates the electrode. At this rate, however, the reaction is predominantly a surface one.

At higher rates of discharge, the only difference in the impedance spectra is in the angle which the loci make to the real axis which decreases from 70 – 60° at the C1 rate. This shows that as the over-voltage is increased so the reaction is driven further into the body of the electrode, and is not confined to the surface as it was at low discharge rates. It also confirms the porous nature of the electrode as the surface films have apparently decreased.

3.4.3. Non-stepwise discharge at the 8, 16 and 23A rates. By non-stepwise we mean $100 \rightarrow 90$, $100 \rightarrow 80$, $100 \rightarrow 70$ and not $100 \rightarrow 90 \rightarrow 80 \rightarrow 70$. When the cells were discharged in this manner, although there were similarities in the impedance spectra (Fig. 9) at different rates of discharging,

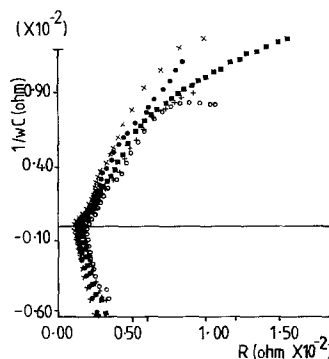


Fig. 9. As for Fig. 7 but discharged at the 8A, C2.875 rate, in non-stepwise manner in the frequency range 10 kHz–1 mHz. \times – 90, \bullet – 30, \blacksquare – 60, $+$ – 100, \circ – 70% states-of-charge.

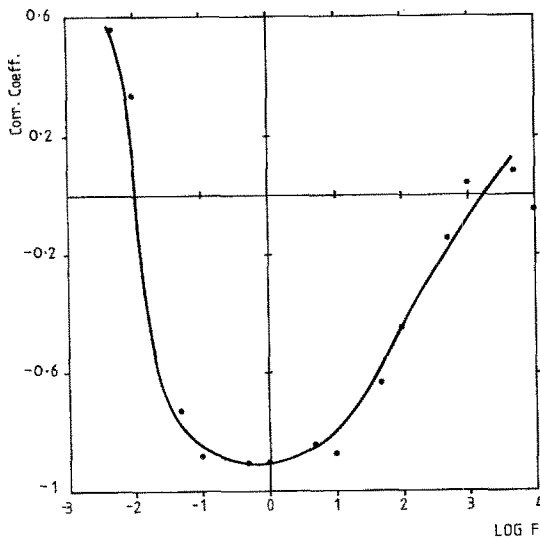


Fig. 10. Plot showing the variation in the correlation coefficient of the capacitive reactance with state-of-charge against log frequency.

there was no trend in the change of the dihedral angle which the loci made to the real axis.

At all rates of discharge, the impedance spectra of a fully discharged cell are similar to those of the charged cells. The only difference is in the magnitude of the resistive and capacitive components. In the fully charged state, the resistive and capacitive components in the frequency range down to 4 mHz are about 7 and 10 mohm while in the fully discharged state they are 50 and 70 mohm.

4. The identification of a state-of-charge test

It was shown earlier that impedance data could be deconvoluted to give an accurate indication of the state-of-charge in certain primary cells [1]. An attempt was made to use impedance measurements to estimate the remaining capacity in secondary aircraft batteries. Unfortunately, the impedance data could not be readily matched to a simple analogue circuit as in the previous cases. As a result, a computer program was written which would search the impedance data files for a possible parameter.

At each state-of-charge and at every frequency, the resistance, capacitive and inductive reactances and total impedance were calculated. The corre-

lation coefficient of each of these components and the state-of-charge was calculated together with the slope and intercept.

From the results of the full analyses for the cell discharged at the C1 rate, it was shown that in Fig. 10 the best state-of-charge parameter could be the capacitive reactance at low frequencies (between 10 and 0.1 Hz), and in this frequency range, the optimum frequency was 0.3931 Hz. This test was significant at least at the 95% level for all of the cells studied. Of the eight cells studied, Fig. 11a shows the mean capacitive reactance of six at 0.39 Hz vs the state-of-charge, whilst Fig. 11b shows the same relationship for the remaining two cells. The mean of the capacitive reactance of the six cells vs the state-of-charge (see Fig. 11a) shows a straight line plot which extends over the complete range of charge and has a slope of about 130% state-of-charge per mohm. The mean capacitive reactance of the experimental two cells vs state-of-charge (Fig. 11b) also shows a linear plot, but the slope of the line in this case is about 210% state-of-charge per mohm.

In view of this result, there are two approaches:

- (a) we can either assume that this result represents the variation which could normally be encountered in these cells. Thus, it was possible to obtain a new mean gradient of about 150% (based on nominal) state-of-charge per mohm, or
- (b) assume that there is a fundamental experimental difference between these cells and the others. In view of the cell-to-cell variation observed care is needed in drawing conclusions about this aspect.

The only measurable difference between these cells was the open circuit voltage. At various states-of-charge the OCVs are shown in Fig. 12. Apart from the low states-of-charge, both plots are parallel but the OCV of one of the cells is 24 mV higher than the corresponding states of the other cells. The reason for this is not clear and requires further investigation.

The open circuit voltage of the cells also show a good correlation with the state-of-charge and could therefore be used to determine the charge remaining in these cells.

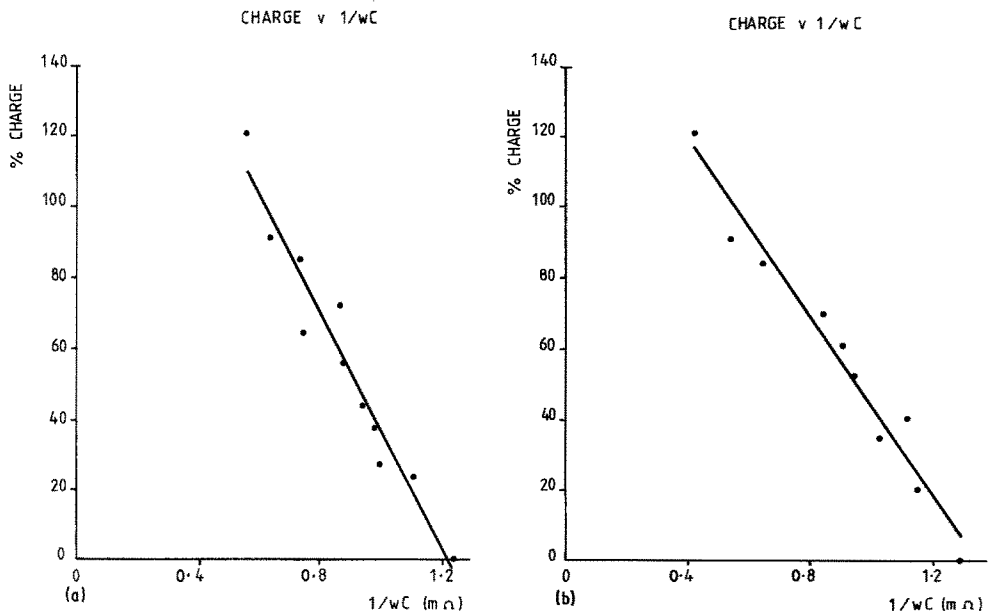


Fig. 11. Using the optimum frequency identified from Fig. 10, Fig. 11a, b shows the two types of relationships identified: (a) mean of the capacitive reactance at 0.3931 Hz for six cells (mohm) with the actual state-of-charge (%); (b) mean of the capacitive reactance at 0.3931 Hz for the remaining 2 cells (mohm) with the actual state-of-charge (%).

5. State-of-charge parameters

From the data accumulated, it can be seen that the state-of-charge of the cell can be determined quite accurately. We do not know if this test

would be valid at other rates of discharge, but the fact that it can be applied to a particular rate itself is encouraging.

The test would be based on two measurements: (a) the open circuit voltage of the cell, and (b) the capacitive reactance of the cell at 0.39 Hz.

For a low capacitive reactance at 0.39 Hz we would expect a high percentage state-of-charge whilst if the capacitive reactance is high the state-of-charge would be expected to be low. As the open circuit voltage vs state-of-charge curve is linear it could be used to confirm our results. This is because apparently anomalous results on one pair of calibration curves might be more correctly suited to the other calibration curves.

The results indicate the difficulties involved in attempting to find an accurate residual capacity test for large (~ 23 Ah) Ni–Cd cells. A clear reason for this is the low impedance of the electrodes which make any change of impedance with discharging difficult to assess. It should be noted that the lower the frequency the greater the difference in impedance between different states-of-charge. This has been made use of in an *ad hoc* tester built for small Ni–Cd cells and which employs effectively a comparison of the capacitive reactance at a sufficiently low frequency in

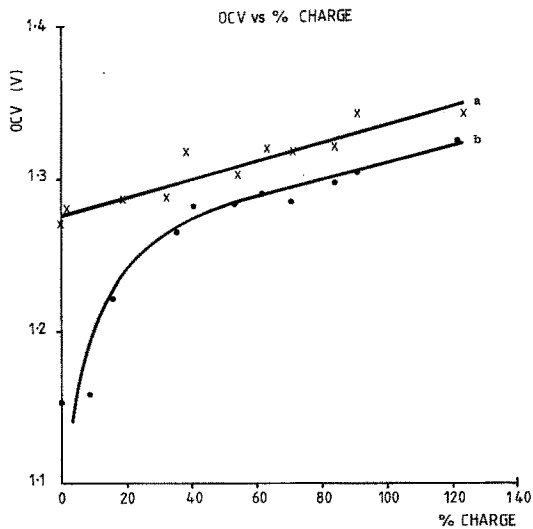


Fig. 12. Variation of the open circuit voltage of the two types of cells identified from the measurement of the capacitive reactance at 0.3931 Hz vs state-of-charge. (a) Corresponds to the cells in Fig. 11a, (b) corresponds to the cells in Fig. 11b.

order to estimate residual cell capacity [12]. (This principle is being extended from very small Ni–Cd cells to 25 Ah cells; the success of this will be reported in due course.) There is good scientific reason for this which will be discussed in a subsequent paper on the individual impedances of mini-electrodes of porous NiO [11]. In this paper we will present the electrochemistry of the individual electrode system.

Acknowledgement

The authors wish to thank the Procurement Executive, Ministry of Defence, for supporting this work. They would also like to thank Dr J. Knight for many constructive ideas and discussions concerning the experimental layout.

References

- [1] N. A. Hampson, S. A. G. R. Karunathilaka R. Leek, T. Haas, M. Hughes, S. A. Cotgreave and L. Greenham, 'The Prediction of the Residual Capacity of Primary Batteries', 3rd Year Report, Department of Chemistry, Loughborough University, December 1981.
- [2] S. A. G. R. Karunathilaka, N. A. Hampson, M. Hughes, W. G. Marshall, R. Leek and T. J. Sinclair, *J. Appl. Electrochem.* **13** (1983) 577.
- [3] S. Lerner, H. Lennon and H. N. Siger, 'Power Sources 3', Edited by D. H. Collins (Oriel Press, Newcastle-upon-Tyne, 1971).
- [4] A. Fleicher, 'Research Studies on the Developing of Testing Methods for Ni–Cd Alkaline Storage Batteries', Final Report, Signal Corps Contract No. DA36-039-SC-42657 (1955).
- [5] K. Kordesch and F. Kornfeil, 'Method and Device for Testing Ni–Cd Batteries', Signal Corps Project No. 162A, Technical Memorandum No. M-1664 (1955).
- [6] K. Kordesch, 'A Method for the Determination of the State-of-Charge of Alkaline Storage Batteries', Signal Corps Project No. 20558, Technical Memorandum No. M-1578 (1964).
- [7] A. Cherdak and R. C. Shair, 'Evaluation of Nickel–Cadmium Battery Testers', Galton Industries, Metuchen, N.J., Signal Corps Contract No. DA36-039-84066 (1961).
- [8] S. Lerner, H. Lennon and H. N. Seiger, 'Power Sources 3', edited by D. H. Collins (Oriel Press, Newcastle-upon-Tyne, 1971).
- [9] S. Sathanarayana, S. Venuyopalan and M. L. Gopikanth, *J. Appl. Electrochem.* **9** (1979) 125.
- [10] A. H. Zimmerman, M. R. Martinelli, M. C. Janecki and C. C. Badcock, *J. Electrochem. Soc.* **129** (1982) 289.
- [11] R. T. Barton, M. Hughes, S. A. G. R. Karunathilaka and N. A. Hampton, unpublished work.
- [12] W. Marshall, R. Leek and N. A. Hampson, *J. Power Sources* **13** (1984) 75.